INVESTIGATIVE NUCLEAR MEDICINE

Radionuclide Cinepneumography: Flow-Volume Imaging of the Respiratory Cycle

Bruce R. Line, Jeffrey A. Cooper, Kenneth M. Spicer, A. Eric Jones, Ronald G. Crystal, and Gerald S. Johnston

National Institutes of Health, Bethesda, Maryland

A procedure is described that generates a series of images spanning an average respiratory cycle. Images are constructed from scintigraphic data with similar respiratory flow and volume characteristics so that they may be displayed in continuous-loop movie format. This technique is noninvasive and requires little patient cooperation or technologist time. It should be most useful in investigations of dynamic pulmonary function, but may be applied to any radionuclide study affected by respiratory motion.

Respiratory motion is well recognized as a factor degrading images of lung, liver, spleen, and kidney (*1–3*). Quantitative phantom studies suggest that respiratory motion doubles the resolution distance for the gamma camera (*1*), and that clinicians using uncorrected images require 50% greater film-density contrast to detect a lesion 2 cm in diameter (*4*).

Several methods have been described to reduce respiratory artifact. Gottschalk and others (*1,5*) have found that breath-holding alone is effective in most resting patients. For dyspneic patients, DeLand (*3*) has described a respiratory gate to produce images from short segments of the breath cycle. Oppenheim (*5*) and Hoffer (*6*) have defined methods that correct for respiratory displacement by keeping the scintigraphic center of the image stationary during data recording. However, it is clear that by removing respiratory motion, these methods discard potentially useful information. For example, clinical experience in cardiac scintigraphy suggests that it is often preferable to have a series of "motion-free" images spanning the dynamic cycle, rather than a single image. Yet, for respiratory motion, few attempts have been made to achieve this end. The technical difficulties largely responsible for this are due to respiratory nonu-

niformity. Cardiac images may be produced by "gated acquisition" procedures because cardiac geometry is relatively uniform during similar phases of regular heart cycles (*7–9*). The lung, however, is not well suited to gated procedures because of inherent variations in breathing pattern, cycle length, and tidal volume (Fig. 1). Even so, lung shape can be characterized by respiratory volume and flow rate. In the procedure to be described, flow and volume data are used to group image information from many cycles into a single average respiratory cycle. We produce a series of images that can be displayed in cine format for study of the dynamics of the lung and other organs affected by respiratory motion.

MATERIALS AND METHODS

A cinepneumographic study requires a gamma camera, a minicomputer, and a pneumotachometer (*10*) that measures airflow at the mouth. Nose clips are used so that all flow to and from the patient passes through a heated pneumotachometer transducer.* To facilitate laminar flow, the transducer is fitted between 10-cm lengths of tapered smooth-walled tubing. This assembly is linear in response (± 4% full scale) to constant flow rates from 0 to 5.5 l/sec and contains 90 ml of dead space. Pneumotachometer output is triggered into an auxiliary nuclide channel of a 7-bit analog-to-digital converter using a 100-Hz logic pulse and a 1-μsec-wide
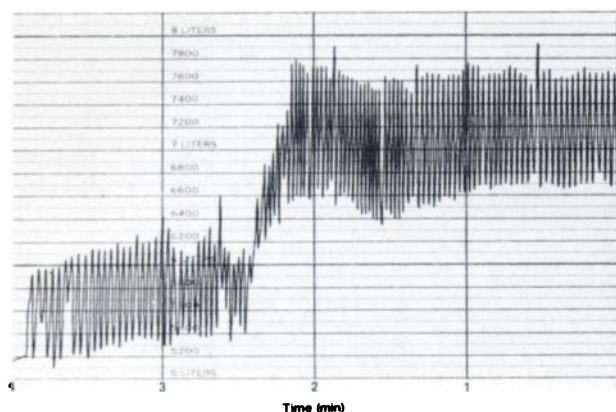
FIG. 1. Volume trace obtained from a spirometer over a 4-min segment of resting tidal ventilation. Volume loss from leakage at patient's mouthpiece is evident near middle of trace. Note considerable variations in breathing pattern, cycle length, and tidal volume.

FIG. 2. Schematic of pneumotachometer and tidal flow-volume loop. Respiratory flow through pneumotachometer tube is proportional to pressure drop across an airflow resistance (R). Differential pressure transducer converts pressure drop (P1 − P2) into analog voltage representing instantaneous flow ($\dot{V}$). Respiratory volume (V) is obtained by integrating instantaneous flow signal. Flow-volume loop is displayed by plotting instantaneous flow (ordinate) versus integrated volume (abcissa). Loop is usually plotted with respect to volume changes in an external reservoir. Reservoir achieves maximum volume at patient's functional residual capacity (FRC) at end of a resting expiration. Flow out of reservoir is "negative" (P1 < P2).
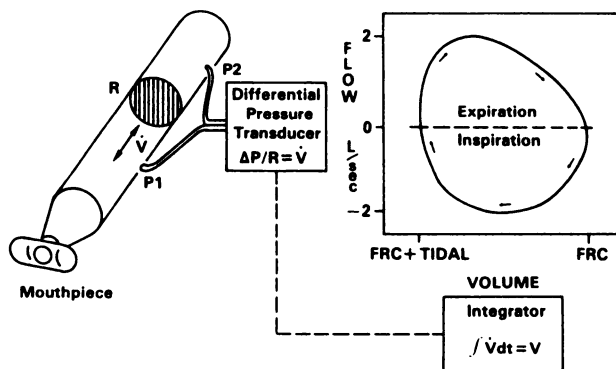
linear gate. The 2–3 million data words stored by the computer during a typical study include list-mode scintillation coordinates, flow values, and 10-msec timing marks. A 16-bit/word minicomputer and a disc-based operating system support the FORTRAN-IV routines used in the analysis and display of the data. In general, studies of 2–3 million words can be fully processed in 4 to 7 min.

PROCEDURE

To sort scintigraphic data among images spanning a respiratory cycle, it is necessary to find a lung geometry "index" that will indicate the image to receive the scintigraphic data. To provide this data-to-image coupling, the index does not need to define the details of lung geometry. Different lung shapes, however, must be associated with different index values; otherwise, an image associated with an index will be blurred by data from several lung configurations.

An index is constructed from respiratory volume and airflow data because lung shape is dependent on both lung volume and the effort of respiratory muscles. A new lung configuration is implied by either a change in lung volume or a change in flow rate at a given lung volume. Accordingly, cycle images are constructed by sorting the scintigraphic data with respect to indices that include both the respiratory volume and the rate of airflow. The method to be described uses a pneumotachometer signal to produce flow-volume (F-V) indices. These associate each 10 msec of scintigraphic data with a cycle image.

An image sequence of an average lung cycle is produced by (a) generating F-V indices from pneumotachometer signals; (b) defining F-V partitions to group the F-V indices by phase of the respiratory cycle; and (c) constructing images from the scintigraphic data in each F-V partition.

F-V index generation. To produce F-V indices, it is necessary to obtain estimates of respiratory airflow and volume. Airflow is proportional to the pressure drop across air channels in the pneumotachometer transducer and can be determined from calibrated transducer output (Fig. 2). Respiratory volume is obtained by integrating the 10-msec airflow values. The F-V index values, which occur during one respiratory cycle, describe a loop because volume and flow vary sinusoidally and differ in phase by about 90°.

Unfortunately, cycle volume calculations are subject to accumulated errors from drifts and transient volume losses (Figs. 1, 3A). Unless these effects are removed, lung shapes will not correspond to constant F-V indices. Drift stems from small biases in the transducer data, from occasional slow leakage at pneumotachometer fittings, and from the physiologic consequences of respiratory gas exchange. The last of these is unavoidable, being related to the respiratory quotient: the ratio of the volumes of carbon dioxide produced to oxygen consumed. This ratio is usually less than one, indicating that more gas is inspired than is expired. The pneumotachometer thus senses a steadily increasing lung volume—clearly an anatomic impossibility. Over many respiratory cycles, mean lung volume approximates a constant value, neither increasing nor decreasing with time. In the absence of drift or leakage artifacts, this should be evident as a constant mean cycle volume during transducer flow integration. In the presence of artifacts, however, the values for mean cycle volume will follow lines with nonzero slopes between points where transient leakage occurs or where slow drifts change. These lines represent the error accumulated to that point in the integration.

220

FIG. 3. (A) Multiple cycles of uncorrected F-V indices. Smearing along volume axis is caused by drift and leakage artifacts. (B) Plots of end-inspiratory (INSP) and end-expiratory (EXP) volume points from a study containing 320 cycles. Original uncorrected volume data (1) and three sets of volume points (2–4) corrected for error using fits with decreasing tolerance. Discarded data associated with atypical cycles are indicated by "break" points (b) between segments of acceptable respiration (see Appendix). Detail of respiratory motion is not changed by volume correction. (C) F-V loops from nine separate error-corrected study segments. Variation in loop intensity is related to number of respiratory cycles in each segment. (D) Summation of corrected F-V loops (C) into a F-V profile. Drift and leakage artifacts present in A are removed.
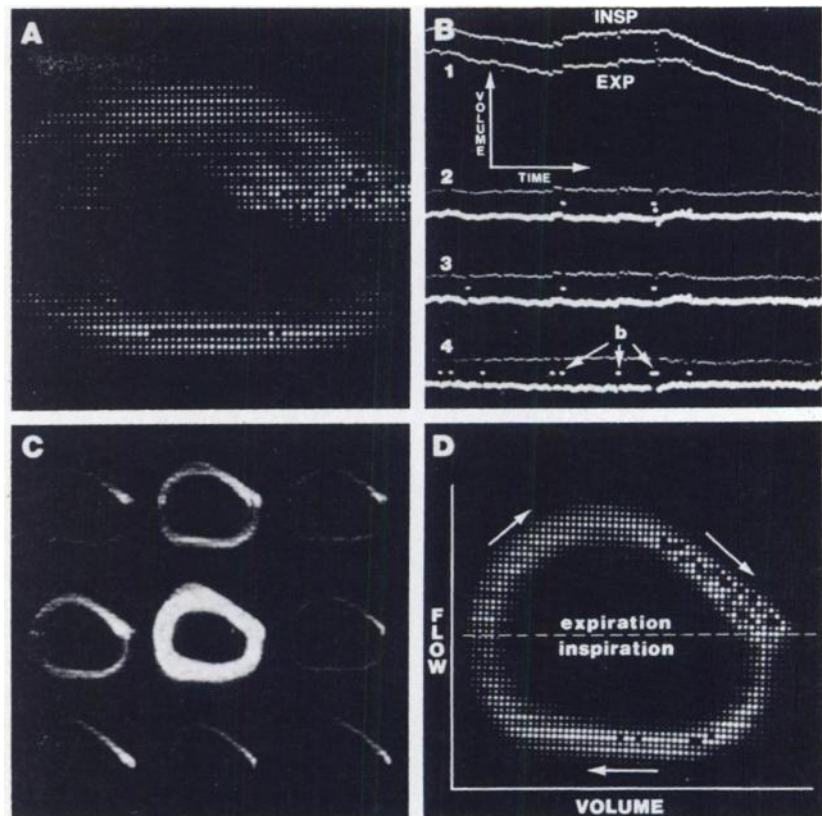
To correct the volume estimates, it is necessary to find the lines of accumulated error and the points of change that best describe the drift and leakage artifacts that have occurred. The procedure used to determine these lines is described in the Appendix. Comparisons of the end-inspiratory and end-expiratory points before and after volume correction (Fig. 3B) indicate that this adjustment preserves respiratory-cycle characteristics but removes drift and leakage artifacts (Figs. 3C, D).

Through correction of each integrated volume estimate by the error indicated on the appropriate error line, pairs of flow and volume values are generated for each 10-msec period of scintigraphic data. These values form the coordinates of an index located on a F-V coordinate grid.

F-V index partitions. Although the data associated with each F-V index could be assigned to a separate image, limitations of counting rate make it desirable to group the data from several F-V indices into each image. Neighboring F-V indices on the F-V grid are associated with similar lung shapes. These shapes can be visualized by dividing the F-V coordinates into F-V partitions and by generating images from the scintigraphic data associated with each partition. Thus, the F-V partition provides the final coupling between the scintigraphic data and the respiratory-cycle images.

It is desirable that the partitions of the F-V coordinate grid lead to a sequence of images spanning an average respiratory cycle. Moreover, the images should represent regional count rates during equal portions of cycle time so that they may be used for quantitative analyses and for cinematic display. To achieve these goals, different partitions must be defined for each patient study because of the wide variation in individual breathing patterns. To define the partitions, the respiratory pattern is recorded by depositing a 10-msec "token" for each F-V index at the appropriate location on the F-V coordinate grid. As each new breath is superimposed on previous respiratory cycles, a F-V profile (Fig. 4) is constructed.
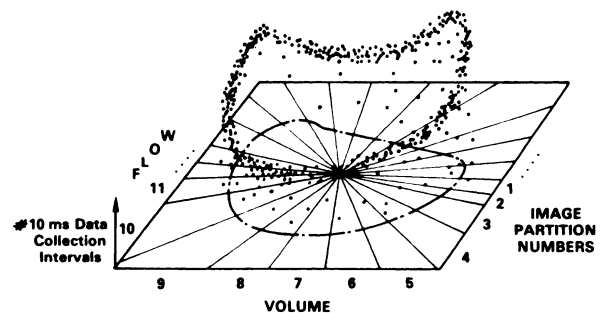
FIG. 4. Schematic of F-V profile and wedge-shaped image partitions. Profile summarizes the breathing pattern during study. Profile height indicates number of 10-msec data-collection intervals at each F-V coordinate. Spread of profile reflects variation in that cycle portion. F-V grid is divided into wedge-shaped regions defining scintigraphic data associated with each image. Wedge size is variable, but each contains same fraction of total imaging time.

The profile is a summary of the breathing pattern during the study. The height of the profile shows the number of 10-msec data-collection intervals associated with each F-V position, whereas the spread of the profile reflects the variation in that portion of the cycle. The time spent in each phase of the cycle is determined by summing the number of 10-msec intervals in that region of the grid.

Wedge-shaped regions converging at the center of the profile (Fig. 4) group similar F-V indices into partitions that span the respiratory cycle. Wedges are generated by a ray, tethered at the center of the F-V profile that sweeps around the grid. Each grid location is assigned the image associated with the current partition as it is passed by the ray. So that each final image may cover an equal fraction of the average cycle time, a new image partition is begun whenever the ray passes enough 10-msec data intervals to exceed the quotient of the total time in the profile divided by the number of desired images. Wedges are generally different in size because the lung does not move at a constant rate, and therefore spends different amounts of time in different phases of the cycle.

The data to be included in each image are now defined by a F-V partition. Although most atypical respiratory cycles are eliminated during generation of the F-V index (see Appendix), it is occasionally desirable to edit the F-V profile to clear portions of cycles that might otherwise degrade the study. This is accomplished by interactively removing the image number associated with each unsuitable F-V index.

Image construction. Images are produced from raw scintigraphic data by matching each 10-msec batch of data with the partition number associated with its F-V index. If the index has not been eliminated by the volume-correction procedure (see Appendix), and the partition number has not been cleared by editing the F-V profile, then the scintigraphic data are added to the image associated with the partition number. This process results in a series of images of 32 × 32 picture elements spanning an average respiratory cycle (Figs. 5 and 6). To ensure that the cine display of the cycle will be free of intensity fluctuations caused by inappropriate amounts of data, each image is linearly adjusted to reflect equal periods of data collection. This correction is necessitated by profile editing, which causes small differences in the number of 10-msec intervals in each partition.

DISCUSSION

A cycle of images spanning an average breath can be generated by sorting scintigraphic data according to respiratory flow and volume. Pneumotachometer flow signals may be integrated and error corrected to yield pairs of flow and volume values for each 10 msec of scintigraphic data. A three-dimensional F-V profile (flow against volume against collection time) is used to characterize the breathing pattern and edit irregular
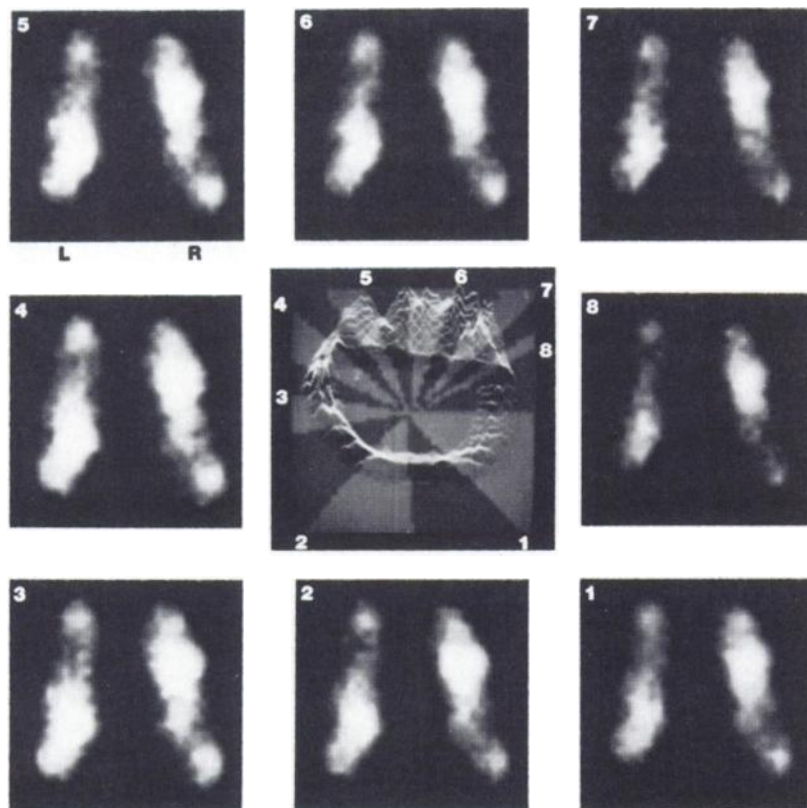
FIG. 5. Final average breath-cycle images of resting respiration in 53-year-old man with emphysema. Tidal volume = 1100 ml. Posterior view of xenon-127 equilibrium ventilation containing total of 2 million counts. F-V profile in center shows most imaging time in prolonged expiratory phase. Image numbers correspond to generating partitions (pairs of light-dark wedges). End-expiration image (No. 8) shows most functional residual capacity in right upper lung and at left base. End-inspiration image (No. 3) demonstrates symmetric lengthening of lungs with poor relative expansion of left upper lobe and of much of right lower lobe.

222
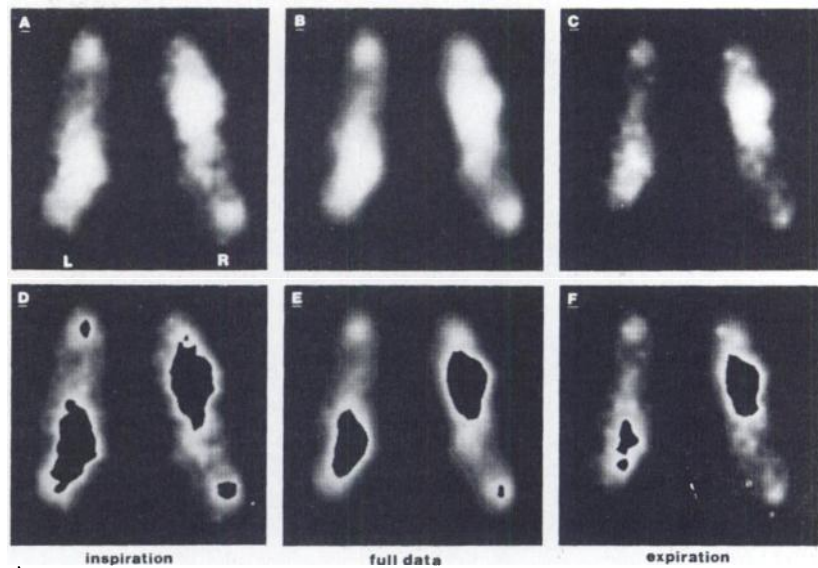
FIG. 6. Comparison of end-cycle and total-data images from patient in Fig. 5. (A) End of tidal inspiration. (B) Full data at one-eighth intensity. (C) End of tidal expiration. Obvious differences between end-cycle images are lost in full-data image. (D–F) Same as A–C except intensities above fixed count threshold are set to zero. Contour shows little change of region in right upper lung but good expansion at left base and fair expansion in left apex and right base.

respiratory cycles. Partitions of this profile define the data associated with each of the cycle images. These images are constructed to study the dynamics of respiratory motion during continuous-loop cinematic display.

The cinepneumographic technique rests on two main assumptions: (a) that shapes of the lung are accurately identified by indices incorporating breath volume and airflow; and (b) that drift and leakage artifacts are adequately corrected by a series of straight lines fitted to mid-cycle volume points. With regard to the first assumption, it it clear that index values need not determine exact lung shape, but must distinguish between different lung shapes. As the number of shapes resolvable in a study increases, the number of scintigraphic events associated with each decreases. Thus, the accuracy required by the index is largely determined by the study's count rate. For example, in studies with 2–3 million scintigraphic events, low counting statistics noticably affect cycles with more than 30 images. Because F-V profiles contain between 800 and 1200 index values, small errors in individual indices should not cause significant classification errors for 30 or fewer images.

The second assumption is central to the method of removing drift and leakage artifacts. These must be removed from integrated volume estimates, because otherwise data previously associated with one image will be misclassified, resulting in image blur. Raw flow data contain little to distinguish these artifacts from voluntary changes in breathing pattern. However, the running integral of respiratory flow reflects the pattern of intrathoracic volume change which, in the absence of drift and leakage artifacts, should oscillate about a constant value. In the presence of artifacts, it is assumed that oscillation will occur about a series of straight lines separated by either leak discontinuities or "elbows" due to changes in the amount of drift. This assumption will

be incorrect for unstable error sources, i.e., for errors that oscillate or change in a complex and rapid fashion. These patterns have not been evident from visual inspection of either the raw or corrected pairs of end-inspiratory and end-expiratory points (Fig. 3B). If they exist, it is likely that they are of small size and therefore should not cause a significant error in image classification.

There are alternative methods of producing images spanning the respiratory cycle. For example, if controlling voluntary efforts and involuntary responses could yield a regular respiratory cycle, then sorting the scintigraphic data by cycle time would produce images of fixed pulmonary geometry. Although studies during artificial respiration are clinically impractical, patients can be trained to breathe regularly or can be guided by visual displays to help stabilize their breathing cycles. However, this imposes demands on technical staff and on patients who may not be capable of changing their respiratory pattern for the length of time required. These problems are magnified when fatigue or dyspnea reduce the attention span. Another alternative to the present method would be to use lung volume alone as an index of lung shape. Lung volume may be estimated from equilibrium count rates in xenon ventilation studies, or more accurately from spirometric data (*11*). Respiratory volume alone is not totally sufficient as an index, however, because at a given lung volume, lung shape is dependent on the effort of respiratory muscle contraction as well as the inspiratory–expiratory phase of the cycle. Errors will arise when different flow rates are lumped into the same volume images—although this may not be a problem in nonquantitative applications. Unfortunately, this method will require a nontrivial procedure to correct for inherent drift and leakage artifacts (Fig. 1).

Cinepneumographic image data should be useful both qualitatively and quantitatively where respiratory motion

is important. When displayed as a movie sequence, cinepneumographic images provide a dynamic view of respiratory function. Details of organ structure, pliability, and parenchymal lesions are likely to be more apparent on cine sequences of "motion-free" images (9,12,13) than on routine "static" views. The cinepneumographic image cycle also can be combined with pneumotachometer measurements of pulmonary tidal volume (Vt_p) and frequency (f_p), to calculate differential bronchospirometric parameters in absolute terms. For example, if the xenon equilibrium count rates at end-inspiration (Cei) and at end-expiration (Cee) are obtained for both lungs (bl) and for each lung separately (l), then the difference between the end-tidal counts (D = Cei − Cee) can be used to estimate the tidal volume of each lung:

$$Vt_l = (D_l/D_{bl})Vt_p,$$

and their minute ventilation ($f_p \times Vt_l$). Moreover, with knowledge of the patient's functional residual capacity (FRC), we can obtain each lung's clearance time (τ_l):

$$\tau_l = \frac{Cee_l}{Cee_{bl}}(FRC)/(f_p \times Vt_l),$$

and fractional exchange per breath, $(f_p \times \tau_l)^{-1}$. Because these values are determined from the equilibrium xenon study, cinepneumography may make it practical to perform repeated estimates, from different views, before and after pharmacologic intervention or during graded exercise.

FOOTNOTE

* Hewlett Packard 21072A, 1.0 l/sec/V.

ACKNOWLEDGMENTS

APPENDIX

The procedure for the correction of respiratory-cycle volume removes drift and leakage artifacts, which cause errors in integrated volume estimates. The average intrathoracic volume is assumed to be constant over many respiratory cycles. But for this volume to be constant, the average respiratory cycle volume must also be constant. Therefore, drifts and leaks can be corrected by keeping the mean volume constant, i.e., by removing the differences determined by fitting the drifts and by removing cycles that are atypical (sighs, coughs, leaks).

Lines representing accumulated error due to these artifacts are determined by least-squares fitting to cycle mid-volume estimates. Mid-volumes are found by averaging adjacent end-inspiratory and end-expiratory volumes. Error line separation points are expected to occur with volume loss, drift fluctuations, and atypical breath cycles. When these are present, the variance of the mid-volume points about the fitted line will increase, implying a poor local fit.

This indicates a need to exclude these data or change the error line. The fitting procedure is controlled by a tolerance value that sets the maximum variance of the mid-volume points about the error lines. If the variance of the mid-volume points about a single fitted line is greater than the tolerance value, then two or more error lines must be produced. An iterative search determines the point separating two lines by repeatedly bisecting the study segment having the greatest variance around its mid-volume regression line. A cycle of data to each side of this point is discarded and the variance of each of the new segments is determined. If any remaining segments exceed tolerance, the process is repeated, producing two or more new error lines for that segment until all segments fall within tolerance.

The tolerance value may be supplied interactively to change the number of lines fitted to the data. The fit is checked by comparing the end-cycle volume points, before and after fitting. Alternatively one can invoke an iterative search that selects a tolerance value by minimizing the number of discarded cycles and the mean difference between the end-inspiratory and end-expiratory volumes taken relative to the mid-volume error lines.

REFERENCES

1. GOTTSCHALK A, HARPER PV, JIMINEZ FF, et al: Quantification of the respiratory motion artifact in radioisotope scanning with the rectilinear focused collimator scanner and the gamma scintillation camera. J Nucl Med 7:243-251, 1966
2. ATKINS HL, HAUSER W, RICHARDS P: Reduction of respiratory artifact in scintillation scanning. Am J Roentgenol 104:682-685, 1968
3. DELAND FH, MAUDERLI W: Gating mechanism for motion-free liver and lung scintigraphy. J Nucl Med 13:939-941, 1972
4. BAIMEL NH, BRONSKILL MJ: Optimization of analog-circuit motion correction for liver scintigraphy. J Nucl Med 19:1059-1066, 1978
5. OPPENHEIM BE: A method using a digital computer for reducing respiratory artifact on liver scans with a camera. J Nucl Med 12:625-628, 1971
6. HOFFER PB, OPPENHEIM BE, STERLING ML, et al: A simple device for reducing motion artifacts in gamma camera images. Radiology 103:199-200, 1972
7. PARKER JA, SECKER-WALKER R, HILL R, et al: A new technique for the calculation of left ventricular ejection fraction. J Nucl Med 13:649-651, 1972
8. GREEN MV, OSTROW HG, DOUGLAS MA, et al: High temporal resolution ECG-gated scintigraphic angiocardiography. J Nucl Med 16:95-98, 1975
9. BACHARACH SL, GREEN MV, BORER JS, et al: A real-time system for multi-image gated cardiac studies. J Nucl Med 18:79-84, 1977
10. FINUCANE KE, EGAN BA, DAWSON SV: Linearity and frequency response of pneumotachographs. J Appl Physiol 32:121-126, 1972
11. KUSHNER TR, LINE BR, BACHARACH SL, et al: A spirometric method for gating xenon ventilation studies. In Proceedings of Seventh Symposium on Sharing of Computer Programs and Technology in Nuclear Medicine, Computer Assisted Data Processing, Atlanta, ERDA CONF-770101. NTIS, Springfield, Va, 1977, pp 207-215
12. ALDERSON PO, VIERAS F, HOUSHOLDER DF, et al: Gated and cinematic perfusion lung imaging in dogs with experimental pulmonary embolism. J Nucl Med 20:407-412, 1979
13. PIAGET: The Mechanisms of Perception. London, Routledge & Kegan Paul, 1969, Chapts., 3-5